Mathematical Modeling of Deformation of Structurally Inhomogeneous Materials Based on a Generalized Rheological Approach

Vladimir M. Sadovskii

Institute of Computational Modelling SB RAS, Krasnoyarsk (Russia)
Department of Computational Mechanics of Deformable Media

sadov@icm.krasn.ru

AMiTaNS'19

Eleventh Conference "Application of Mathematics in Technical and Natural Sciences"

Albena (Bulgaria), 20 – 25 June 2019

Contents

Variational inequalities

Minimization of a convex function on a convex set

$$f(u) = \min_{\tilde u \in F} f(\tilde u) \qquad \Longleftrightarrow \qquad (\tilde u - u) \cdot \nabla f(u) \geqslant 0 \quad \forall\, \tilde u \in F$$

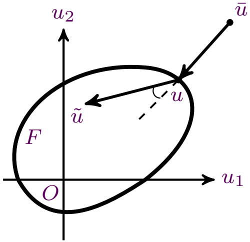

Simple example

A projection $u = \pi(\bar u)$ onto the convex and closed set:

$$f(u) = \|u - \bar u\|^2, \qquad \nabla f(u) = 2\,(u - \bar u)$$

$$u \in F: \qquad (\tilde u - u) \cdot (u - \bar u) \geqslant 0 \quad \forall\, \tilde u \in F$$

Variational inequality for monotone operator $Q(u) \neq \nabla f(u)$:

$$(\tilde u - u) \cdot Q(u) \geqslant 0, \quad u,\, \tilde u \in F$$

It has a unique solution if F is convex closed set and if $Q(u)$ is strongly monotone:

$(u' - u) \cdot \big(Q(u') - Q(u)\big) \geq \alpha^2 \|u' - u\| \quad \forall\, u,\, u' \in F \ (\alpha \neq 0)$

The Mises principle of maximal plastic power

A power of plastic dissipation achieves maximum on actual stresses:

$$\boldsymbol{\sigma} : \boldsymbol{e}^p \geqslant \tilde{\boldsymbol{\sigma}} : \boldsymbol{e}^p, \quad \boldsymbol{\sigma}, \tilde{\boldsymbol{\sigma}} \in F \qquad \Big(-(\tilde{\boldsymbol{\sigma}} - \boldsymbol{\sigma}) : \boldsymbol{e}^p \geq 0 \Big)$$

Application of Kuhn–Tucker's theorem

$$F = \Big\{ \boldsymbol{\sigma} \;\Big|\; f_j(\boldsymbol{\sigma}) \leqslant 0 \quad (j = 1, \ldots, k) \Big\}, \qquad L(\boldsymbol{\sigma}, \lambda) = \boldsymbol{\sigma} : \boldsymbol{e}^p + \sum_{j=1}^{k} \lambda_j \, f_j(\boldsymbol{\sigma})$$

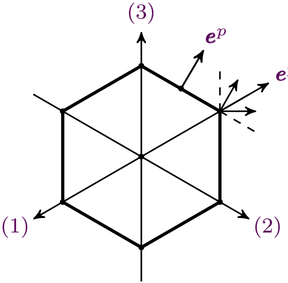

Associative plastic flow rule:

$$\boldsymbol{e}^p = \sum_{j=1}^{k} \lambda_j \frac{\partial f_j(\boldsymbol{\sigma})}{\partial \boldsymbol{\sigma}}, \qquad \lambda_j \geqslant 0, \quad \lambda_j \, f_j(\boldsymbol{\sigma}) = 0$$

Complete system of the theory of elastic-plastic Prandtl–Reuss flow theory:

$$\rho \frac{\partial v}{\partial t} = \nabla \cdot \boldsymbol{\sigma} + \rho g, \qquad \boldsymbol{e}^p = \frac{1}{2} (\nabla v + \nabla v^*) - \boldsymbol{a} : \frac{\partial \boldsymbol{\sigma}}{\partial t}, \qquad (\tilde{\boldsymbol{\sigma}} - \boldsymbol{\sigma}) : \boldsymbol{e}^p \geqslant 0$$

Elastic Cosserat continuum

The complete system of equations contains the equations of translational and rotational motion, kinematic and constitutive equations.

$$\rho\,\frac{\partial v}{\partial t} = \nabla\cdot\boldsymbol{\sigma} + \rho\,g, \quad j\,\frac{\partial\omega}{\partial t} = \nabla\cdot\boldsymbol{m} - 2\,\sigma^a + j\,q$$
$$\frac{\partial\boldsymbol{\Lambda}}{\partial t} = \nabla v + \boldsymbol{\omega}, \quad \frac{\partial\boldsymbol{M}}{\partial t} = \nabla\omega$$
$$\boldsymbol{\sigma} = \lambda\,(\boldsymbol{\delta} : \boldsymbol{\Lambda}^s)\,\boldsymbol{\delta} + 2\,\mu\,\boldsymbol{\Lambda}^s + 2\,\alpha\,\boldsymbol{\Lambda}^a$$
$$\boldsymbol{m} = \beta\,(\boldsymbol{\delta} : \boldsymbol{M}^s)\,\boldsymbol{\delta} + 2\,\gamma\,\boldsymbol{M}^s + 2\,\eta\,\boldsymbol{M}^a$$

Hyperbolicity conditions

$$3\,\lambda + 2\,\mu > 0, \quad \mu,\ \alpha > 0; \qquad 3\,\beta + 2\,\gamma > 0, \quad \gamma,\ \eta > 0$$

Velocities of elastic waves

$$c_p = \sqrt{\frac{\lambda + 2\,\mu}{\rho}}, \quad c_s = \sqrt{\frac{\mu + \alpha}{\rho}}, \quad c_m = \sqrt{\frac{\beta + 2\,\gamma}{j}}, \quad c_\omega = \sqrt{\frac{\gamma + \eta}{j}}$$

- v – velocity vector, ω – vector of angular velocity, j – moment of inertia of particles
- $\boldsymbol{\sigma}$ – stress tensor, $\boldsymbol{m}$ – tensor of couple stresses
- $\boldsymbol{\Lambda}$ and $\boldsymbol{M}$ – tensors of strain and curvature, g and q – mass forces and couple forces
- λ, μ, α, β, γ, η – phenomenological parameters

Matrix form of the equations

Thermodynamically consistent equations of the theory of elasticity:

$$A\,\frac{\partial U}{\partial t} = \sum_{i=1}^{n} B^i\,\frac{\partial U}{\partial x_i} + Q\,U + G$$

When taking into account plastic deformation, the system replaced by a variational inequality:

$$(\widetilde{U} - U)\cdot\Big(A\,\frac{\partial U}{\partial t} - \sum_{i=1}^{n} B^i\,\frac{\partial U}{\partial x_i} - Q\,U - G\Big) \geqslant 0, \qquad \widetilde{U},\ U \in F$$

- F – convex and closed set determined by yield criterion
- $U(t,x)$ – m-vector of unknown functions, $\widetilde{U}$ – a variable vector
- A – symmetric positive definite matrix of coefficients before time derivatives
  B^i – symmetric matrices of coefficients before derivatives with respect to spatial variables
  Q – antisymmetric matrix, G – vector of bulk forces and prestresses
- n – spatial dimension of the problem (1, 2 or 3)
- dimension m of the system and the specific type of matrices–coefficients determined by the used mathematical model

Generalised solutions

Variational inequality for a thermodynamically consistent hyperbolic operator of Godunov's type:

$$(\widetilde{U} - U) \cdot \left(\frac{\partial \varphi(U)}{\partial t} - \sum_{i=1}^{n} \frac{\partial \psi_i(U)}{\partial x_i} - G \right) \geqslant 0, \qquad \widetilde{U},\ U \in F$$

$$\varphi(U) = \frac{\partial \Phi(U)}{\partial U}, \qquad \psi_i(U) = \frac{\partial \Psi_i(U)}{\partial U}$$

Fizmatlit, 1997

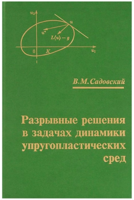

Divergent form of variational inequality:

$$\widetilde{U} \cdot \left(\frac{\partial \varphi(U)}{\partial t} - \sum_{i=1}^{n} \frac{\partial \psi_i(U)}{\partial x_i} - G \right) \geqslant \frac{\partial}{\partial t} \Big(U \cdot \varphi(U) - \Phi(U) \Big) -$$

$$- \sum_{i=1}^{n} \frac{\partial}{\partial x_i} \Big(U \cdot \psi_i(U) - \Psi_i(U) \Big) - U \cdot G, \qquad \widetilde{U},\ U \in F$$

- Strong discontinuity relations
- Uniqueness of the solution of the Cauchy problem
- Continuous dependency on initial data
- Correctness of setting dissipative boundary conditions

Differently resistant materials

The most part of natural and especially artificial materials have different resistance in tension and compression:
– metal foams
– fiber reinforced composites
– granular materials
– soils
– rocks
– etc.
Hence, this property must be taken into account under mathematical modeling.

Experimental study

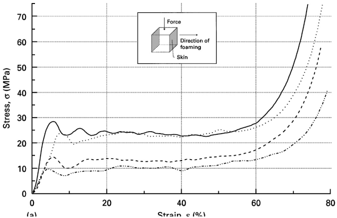

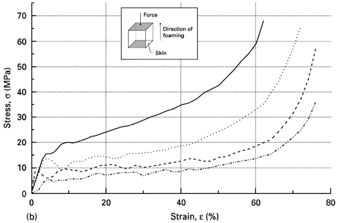

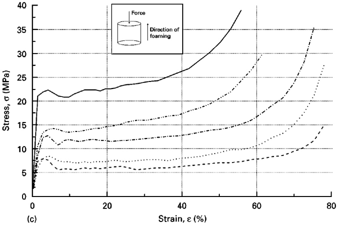

J. Banhart, J. Baumeister. **Deformation characteristics of metal foams.** *J. Mater. Sci.*, **33**(6): 1431–1440, 1998.

Constitutive relations of a rigid contact

Springer, 2012

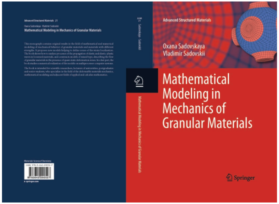

http://link.springer.com/book/10.1007/978-3-642-29053-4

Downloads – **10502**

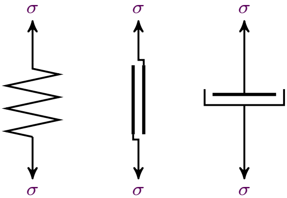

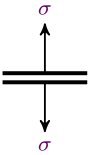

$$\sigma \leqslant 0, \quad \varepsilon \geqslant 0, \quad \sigma\varepsilon = 0 \quad \Leftrightarrow \quad \begin{cases} (\tilde{\sigma} - \sigma) : \varepsilon \leqslant 0 & \sigma,\ \tilde{\sigma} \leqslant 0 \\ (\tilde{\varepsilon} - \varepsilon) : \sigma \leqslant 0 & \varepsilon,\ \tilde{\varepsilon} \geqslant 0 \end{cases}$$

$$(\tilde{\boldsymbol{\sigma}} - \boldsymbol{\sigma}) : \boldsymbol{\varepsilon} \leqslant 0 \quad \boldsymbol{\sigma},\ \tilde{\boldsymbol{\sigma}} \in \boldsymbol{K} \quad \Leftrightarrow \quad (\tilde{\boldsymbol{\varepsilon}} - \boldsymbol{\varepsilon}) : \boldsymbol{\sigma} \leqslant 0 \quad \boldsymbol{\varepsilon},\ \tilde{\boldsymbol{\varepsilon}} \in \boldsymbol{C}$$

$$\boldsymbol{K} = \{\boldsymbol{\sigma} \mid \boldsymbol{\sigma} : \boldsymbol{\varepsilon} \leqslant 0 \ \text{ for all } \ \boldsymbol{\varepsilon} \in \boldsymbol{C}\} \quad \Leftrightarrow \quad \boldsymbol{C} = \{\boldsymbol{\varepsilon} \mid \boldsymbol{\sigma} : \boldsymbol{\varepsilon} \leqslant 0 \ \text{ for all } \ \boldsymbol{\varepsilon} \in \boldsymbol{K}\}$$

Rheological schemes of elastic-plastic granular materials

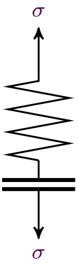

ideal granular material with elastic particles

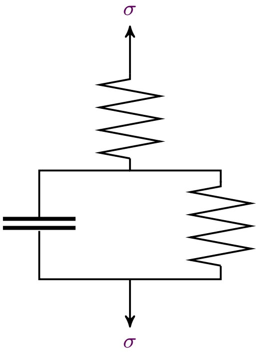

heteromodular elastic material

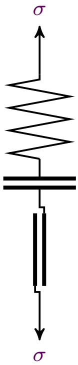

elastic-plastic granular material

Rheological schemes with 3 elements: elastic spring, rigid contact, plastic hinge

Rheological schemes of viscoelastic granular materials

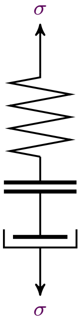

viscoelastic granular material
(Maxwell model)

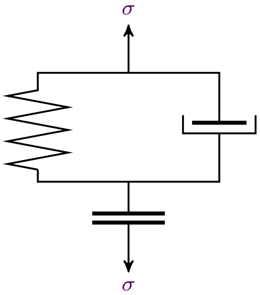

viscoelastic granular material
(Kelvin–Voigt model)

Rheological schemes with 3 elements: elastic spring, viscous damper and rigid contact

Rheological schemes of porous materials

In this way we construct the models of porous materials taking into account elastic, plastic and viscous properties.

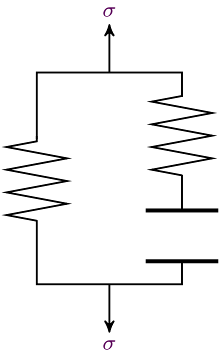

elastic porous medium

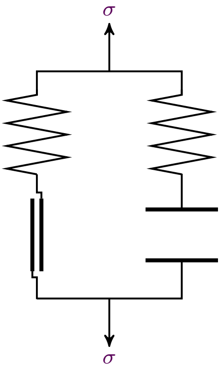

elastic-plastic porous medium

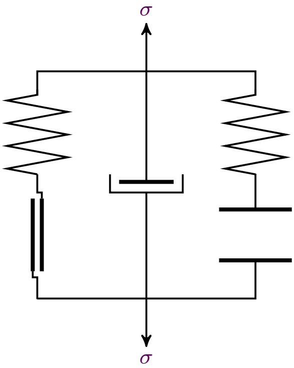

elastic-viscoplastic porous medium

Modeling of granular media

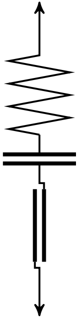

Strain tensor $\boldsymbol{\varepsilon} = \boldsymbol{\varepsilon}^e + \boldsymbol{\varepsilon}^c + \boldsymbol{\varepsilon}^p$

The inequality of Haar and Karman

$$(\tilde{\boldsymbol{\sigma}} - \boldsymbol{\sigma}) : \bigl(\boldsymbol{a} : \boldsymbol{\sigma} - \boldsymbol{\varepsilon}^e - \boldsymbol{\varepsilon}^c\bigr) \geqslant 0, \qquad \boldsymbol{\sigma},\ \tilde{\boldsymbol{\sigma}} \in K$$

By the definition of the projection it means

$$\boldsymbol{\sigma} = \pi_a\bigl(\boldsymbol{a}^{-1} : (\boldsymbol{\varepsilon}^e + \boldsymbol{\varepsilon}^c)\bigr)$$

The Mises inequality $(\tilde{\boldsymbol{\sigma}} - \boldsymbol{\sigma}) : \dot{\boldsymbol{\varepsilon}}^p \leqslant 0, \qquad \boldsymbol{\sigma},\ \tilde{\boldsymbol{\sigma}} \in F$

Equations of motion $\rho\, \dot{v} = \nabla \cdot \boldsymbol{\sigma} + \rho\, g$

Kinematic equations $2\dot{\boldsymbol{\varepsilon}} = \nabla v + (\nabla v)^*$

The set F of admissible variations is defined by the Mises yield condition: $F = \Bigl\{\boldsymbol{\sigma}\ \Big|\ \tau(\boldsymbol{\sigma}) \leqslant \tau_s\Bigr\}$. As a convex cone K of stresses, allowed by the strength criterion, the Mises–Schleicher circular cone $K = \Bigl\{\boldsymbol{\sigma}\ \Big|\ \tau(\boldsymbol{\sigma}) \leqslant æ\, p(\boldsymbol{\sigma})\Bigr\}$ is used.

- $\boldsymbol{\sigma}$ – stress tensor, $\boldsymbol{\varepsilon}$ – strain tensor: $\boldsymbol{\varepsilon}^e$, $\boldsymbol{\varepsilon}^c$, $\boldsymbol{\varepsilon}^p$ – elastic, granular and plastic parts
- $\tau(\boldsymbol{\sigma})$ – intensity of tangential stresses, $p(\boldsymbol{\sigma})$ – hydrostatic pressure
- τ_s – yield point of particles, æ – parameter of internal friction

Porous materials

Elastic material

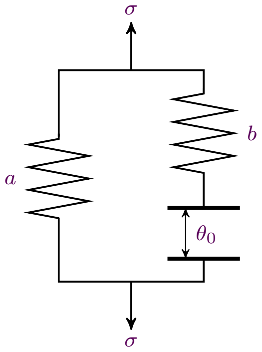

Rheological scheme

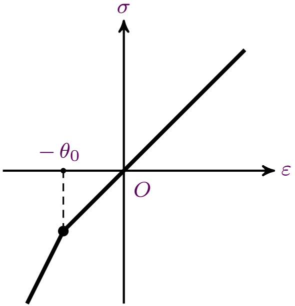

Diagram of tension–compression

The behavior of a material in tension and in compression before the collapse of pores is simulated by an elastic spring with given compliance modulus a, and the increase in stiffness after collapse is simulated by an additional spring with the compliance modulus b.
A diagram of uniaxial tension–compression of a porous material is represented as a two-segment broken line.
Such scheme describes the elastic process that occurs without dissipation of mechanical energy.

Porous materials

Elastic-plastic material

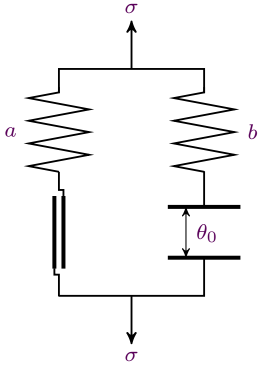

Rheological scheme

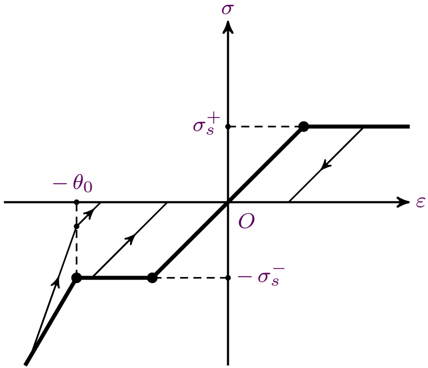

Diagram of tension–compression

Under the tensile stress σ_s^+ a skeleton goes into the state of plastic flow, and under the compressive stress $-\,\sigma_s^-$ the plastic loss of stability takes place. The stage of elastic-plastic deformation of a solid material after the collapse of pores is described by the rheological scheme of linear hardening. A diagram of uniaxial tension–compression is represented as a four-segment broken line.

Complete system of equations

Mathematical model has the form:

$$\rho\,\dot{v} = \nabla\cdot\boldsymbol{\sigma} + f$$

$$(\tilde{\boldsymbol{s}} - \boldsymbol{s}) : (\boldsymbol{a} : \dot{\boldsymbol{s}} - \nabla v) \geqslant 0, \qquad \tilde{\boldsymbol{s}},\ \boldsymbol{s} \in F$$

$$\boldsymbol{b} : \dot{\boldsymbol{q}} = \frac{1}{2}\,(\nabla v + \nabla v^*), \qquad \boldsymbol{\sigma} = s + \pi_K(\boldsymbol{q} + \boldsymbol{q}^0)$$

- $\rho = \rho_0\,(1 - \theta_0)$ – initial density, v – velocity vector
- ∇ – vector of gradient with respect to spatial variables
- f is the vector of bulk forces

Vector v, tensors $\boldsymbol{s}$ and $\boldsymbol{q}$ are unknown functions in this model.

This system can be written in matrix form as a variational inequality:

$$(\widetilde{V} - V)\cdot\left(A\,\frac{\partial U}{\partial t} - \sum_{i=1}^{n} B^i\,\frac{\partial V}{\partial x_i} - Q\,V - G\right) \geqslant 0, \qquad \widetilde{V},\ V \equiv \pi_K(U) \in F$$

- F – convex and closed set determined by yield criterion
- $U(t,x)$ – m-vector of unknown functions, $\widetilde{U}$ – a variable vector
- A – symmetric positive definite matrix of coefficients before time derivatives,
  B^i – symmetric matrixes of coefficients before derivatives with respect to spatial variables
  Q – antisymmetric matrix, G – vector of bulk forces and prestresses
- n – spatial dimension of the problem (1, 2 or 3)
- dimension m of the system and the specific type of matrices–coefficients determined by the used mathematical model

Numerical algorithm

- The algorithm of numerical implementation of mathematical models is explicit in time and is constructed by means of the splitting method with respect to physical processes in the following way:
  - first, the elastic problem is solved at each time step
  - next, the obtained solution is corrected to take into account plastic and granular properties of a material
- For the solution of elastic problem the two-cyclic splitting method with respect to the spatial variables is used
- One-dimensional hyperbolic systems of equations of the form

$$A\,\frac{\partial U^k}{\partial t} = B^i\,\frac{\partial U^k}{\partial x_i} + G^i$$

($k = \overline{1, 2\,n}$ – the number of the splitting stage, $i = \overline{1, n}$ – the direction of splitting) in spatial directions are solved by means of the monotone finite-difference ENO–scheme of the "predictor–corrector" type; piecewise-linear splines, discontinuous at the boundaries of meshes, are constructed by a special procedure of limit reconstruction, which enables one to improve an accuracy of a numerical solution

- Plasticity and granularity of materials are taken into account by means of a special algorithms for the correction of stresses, used in computations

Structure of parallel program

Computational algorithm is implemented as a parallel program system for the solution of dynamic problems in structurally inhomogeneous deformable materials on multiprocessor computers by means of the SPMD technology in Fortran using the MPI library.

1. Preprocessor program
   - grid generation
   - uniform distribution of initial data between parallel computational nodes
   - packing of its part of data in binary files of direct access by each node of a cluster
2. Main program
   - step-by-step numerical computation of a problem on each node of a cluster
   - data exchange between the processes
   - special conservation of resulting data in the control points

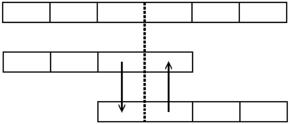

The scheme of exchange with contour meshes

3. Postprocessor program
   - compression of files, containing the results of computations in the control points
   - graphical representation of results

Registration of programs in Rospatent

Parallel program systems for the solution of two-dimensional and three-dimensional elastic-plastic problems of the dynamics of granular media

Certificates of state registration of computer programs no. 2012613989 and 2012613990 from 28.04.2012

РОССИЙСКАЯ ФЕДЕРАЦИЯ

СВИДЕТЕЛЬСТВО

о государственной регистрации программы для ЭВМ

№ 2012613989

«Программный комплекс для решения двумерных упругопластических задач динамики сыпучих сред (2Dyn_Granular)»

Правообладатель(ли): *Федеральное государственное бюджетное учреждение науки Институт вычислительного моделирования Сибирского отделения Российской академии наук (RU)*

Автор(ы): *Садовский Владимир Михайлович, Садовская Оксана Викторовна (RU)*

Заявка № 2012610982

Дата поступления 14 февраля 2012 г.

Зарегистрировано в Реестре программ для ЭВМ *28 апреля 2012 г.*

Руководитель Федеральной службы по интеллектуальной собственности

Б.П. Симонов

РОССИЙСКАЯ ФЕДЕРАЦИЯ

СВИДЕТЕЛЬСТВО

о государственной регистрации программы для ЭВМ

№ 2012613990

«Программный комплекс для решения трёхмерных упругопластических задач динамики сыпучих сред (3Dyn_Granular)»

Правообладатель(ли): *Федеральное государственное бюджетное учреждение науки Институт вычислительного моделирования Сибирского отделения Российской академии наук (RU)*

Автор(ы): *Садовский Владимир Михайлович, Садовская Оксана Викторовна (RU)*

Заявка № 2012610988

Дата поступления 14 февраля 2012 г.

Зарегистрировано в Реестре программ для ЭВМ *28 апреля 2012 г.*

Руководитель Федеральной службы по интеллектуальной собственности

Б.П. Симонов

Programs: 2Dyn_Granular, 3Dyn_Granular

Parallel program systems for the solution of two-dimensional and three-dimensional dynamic problems of the Cosserat elasticity theory

Certificates of state registration of computer programs no. 2012614823 and 2012614824 from 30.05.2012

РОССИЙСКАЯ ФЕДЕРАЦИЯ

СВИДЕТЕЛЬСТВО

о государственной регистрации программы для ЭВМ

№ 2012614823

«Программный комплекс для расчёта двумерных динамических задач моментной теории упругости (2Dyn_Cosserat)»

Правообладатель(ли): *Федеральное государственное бюджетное учреждение науки Институт вычислительного моделирования Сибирского отделения Российской академии наук (RU)*

Автор(ы): *Садовский Владимир Михайлович, Садовская Оксана Викторовна, Варыгина Мария Петровна (RU)*

Заявка № 2012611061

Дата поступления 16 февраля 2012 г.

Зарегистрировано в Реестре программ для ЭВМ *30 мая 2012 г.*

Руководитель Федеральной службы по интеллектуальной собственности

Б.П. Симонов

РОССИЙСКАЯ ФЕДЕРАЦИЯ

СВИДЕТЕЛЬСТВО

о государственной регистрации программы для ЭВМ

№ 2012614824

«Программный комплекс для расчёта трёхмерных динамических задач моментной теории упругости (3Dyn_Cosserat)»

Правообладатель(ли): *Федеральное государственное бюджетное учреждение науки Институт вычислительного моделирования Сибирского отделения Российской академии наук (RU)*

Автор(ы): *Садовский Владимир Михайлович, Садовская Оксана Викторовна, Варыгина Мария Петровна (RU)*

Заявка № 2012611062

Дата поступления 16 февраля 2012 г.

Зарегистрировано в Реестре программ для ЭВМ *30 мая 2012 г.*

Руководитель Федеральной службы по интеллектуальной собственности

Б.П. Симонов

Programs: 2Dyn_Cosserat, 3Dyn_Cosserat

Program systems 2Dyn_Granular, 3Dyn_Granular are intended for numerical realization of the universal mathematical model, describing small strains of elastic, plastic and granular materials.
Program systems 2Dyn_Cosserat, 3Dyn_Cosserat allows to solve numerically dynamic problems of the moment elasticity, taking into account rotations of the particles of microstructure of a material.
On interblock boundaries of blocks the conditions of continuity of the velocity vectors and the stress vectors are placed. On external boundaries of computational domain the main types of dissipative boundary conditions in terms of velocities, stresses or mixed boundary conditions, or symmetry conditions, ensuring mathematical correctness of a problem, can be specified.

Distribution of computational load

Two-dimensional case

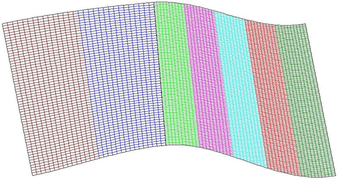

Decomposition of a medium body, consisting of 2 blocks, between 7 processes

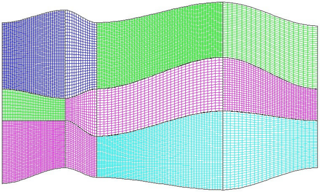

Decomposition of a medium body, consisting of 12 blocks, between 4 processes

Three-dimensional case

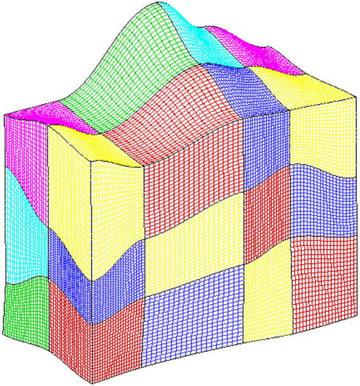

Decomposition of a medium body, consisting of 24 blocks, between 24 processes

Lamb's problem for a medium with rigid inclusion

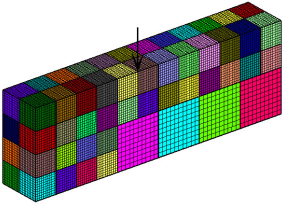

Distribution of computational domain between processors

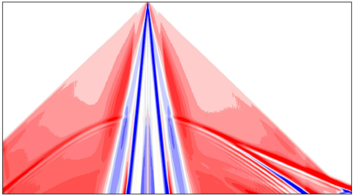

Seismogram of the displacement u_1

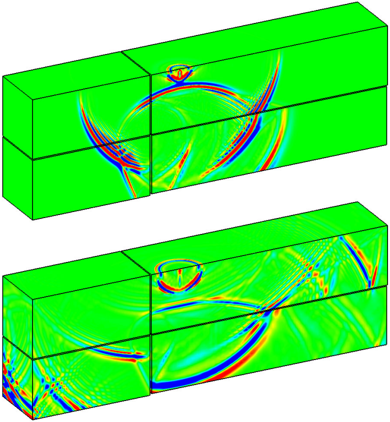

Level surfaces of the stress σ_{11}

The elastic medium body consists of two layers. Elasticity parameters of a compact ground are defined in upper layer and in part of lower layer, parameters of a strong rock are defined in remaining part of lower layer. 4 blocks, 68 processors: 64 – in a compact ground, 4 – in a strong rock, grid dimension for each processor is $50 \times 50 \times 50$ meshes.

Natural resonance of the Cosserat medium

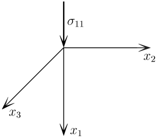

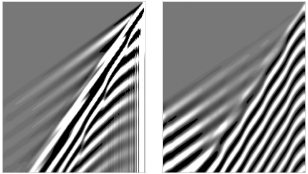

Seismograms of incident waves: impulsive loading (left) and periodic loading (right)

$$\sigma_{11} = -p_1^* \delta(x)\, \sin(2\pi\nu t)$$

synthetic polyurethane

64 processors

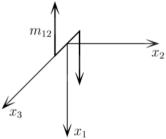

$$m_{12} = -q_2^* \delta(x)\, \sin(2\pi\nu t)$$

Periodic loading: level surfaces of angular velocity ω_2 for nonresonance frequency (left) and resonance frequency (right)

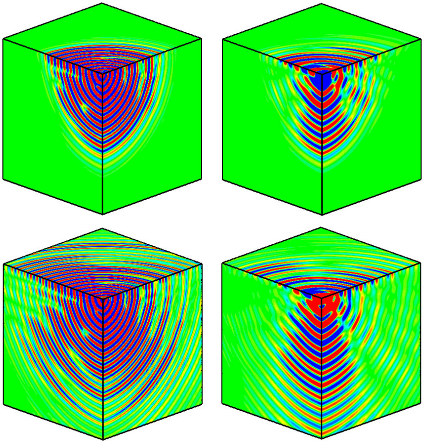

$\nu = 1.5\,\nu_*$ $\qquad$ $\nu = \nu_* = 1/T$

Exact solutions: Low porosity

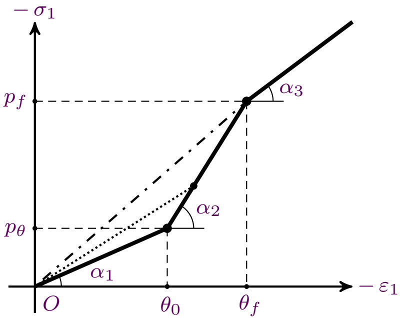

In a low-porous material with relatively high yield point, where $\theta_0 \leqslant \theta_f \equiv \tau_s/\mu_a$, pore collapse under the action of compressive stresses takes place at the stage of elastic deformation, and plasticity shows itself only after compaction of a medium.

On a shock wave, that travels with a velocity c in the direction of x_1 axis, in a general case the dynamic and kinematic equations and their corollary are fulfilled:

$$\rho\, c\,(v_1^+ - v_1^-) + \sigma_1^+ - \sigma_1^- = 0, \quad c\,(\varepsilon_1^+ - \varepsilon_1^-) + v_1^+ - v_1^- = 0, \quad \rho\, c^2 = \frac{\sigma_1^+ - \sigma_1^-}{\varepsilon_1^+ - \varepsilon_1^-}$$

Here the values with a superscript "+" are related with the state behind the wave front, and the values with a superscript "–" are related with the state ahead the wave front.

$$c_p^0 = \sqrt{\frac{k_a + 4\,\mu_a/3}{\rho}}, \quad c_\theta = c_p\sqrt{\frac{p_0}{p_0 + k_b\,\theta_0}} \quad \left(c_p = \sqrt{\frac{k_a + k_b + 4\,\mu_a/3}{\rho}}\right), \quad c_f = \sqrt{\frac{k_a + k_b}{\rho}}$$

Exact solutions: High porosity

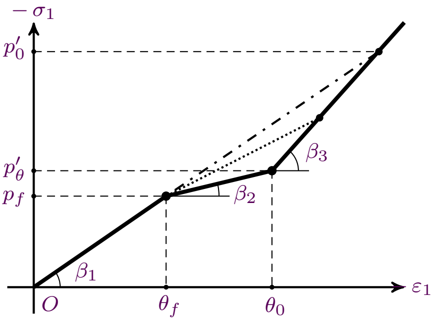

In a material with low yield point and high porosity, where $\theta_0 > \theta_f \equiv \tau_s/\mu_a$, plasticity sets in before the state of compaction. This scenario corresponds to the uniaxial diagram, which is shown in the figure.

In this case the characteristic wave velocities are velocities of elastic and plastic waves:

$$c_p^0 = \sqrt{\frac{k_a + 4\,\mu_a/3}{\rho}}, \quad c_f^0 = \sqrt{\frac{k_a}{\rho}}$$

the velocity of wave of plastic compaction and the velocity of solitary elastic-plastic wave of compaction (for very high pressure):

$$c_\theta' = c_f \sqrt{\frac{p_0 - p_f'}{p_0 - p_f' + k_b\,(\theta_0 - \tau_s/\mu_a)}}, \quad c_0' = c_f \sqrt{\frac{p_0}{p_0 + k_b\,\theta_0 - 4\,\tau_s/3}}$$

Tree of the solutions

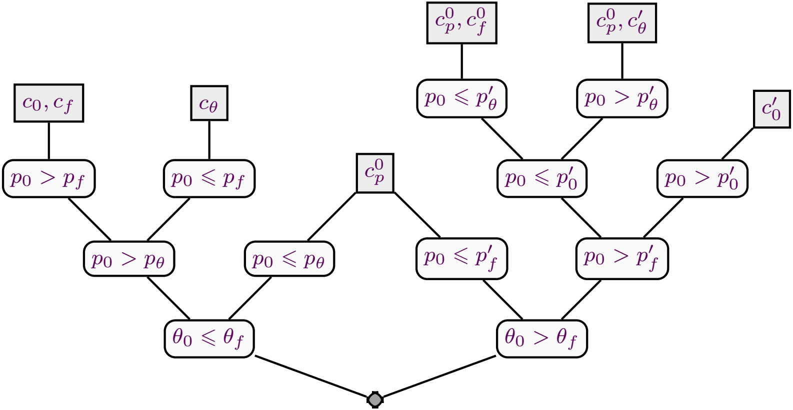

The complete tree of the solutions is shown in this figure as a graph with the vertices specifying velocities of one or two waves depending on the solution variant.

$$p_\theta = (k_a + 4\,\mu_a/3)\,\theta_0, \quad p_f = 4\,\tau_s/3 + (k_a + k_b)\,\tau_s/\mu_a - k_b\,\theta_0$$

$$p_f' = (4/3 + k_a/\mu_a)\,\tau_s, \quad p_\theta' = k_a\,\theta_0 + 4\,\tau_s/3, \quad p_0' = \Big(k_b + \frac{4}{3}\,\mu_a\Big)\,\frac{3\,k_b\,\theta_0 - 4\,\tau_s}{3\,k_b - 4\,\mu_a}$$

Comparison of the solutions

Graphs of normal stress in the case of low porosity ($\theta_f = 0.15\,\%$).

The elastic wave of compaction (i. e., the shock-wave transition of pores into the collapse state) and usual plastic wave as in a compacted material without pores are realized in this case.

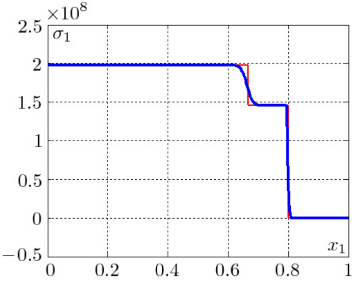

$\theta_0 = 0.1\,\%,\ \ p_0 = 5\,\tau_s$

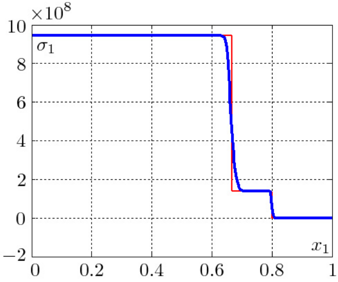

$\theta_0 = 1\,\%,\ \ p_0 = 25\,\tau_s$

Comparison of the solutions

Graphs of normal stress in the case of high porosity ($\theta_f = 0.15\,\%$).

In this case the usual elastic precursor in a porous material and plastic wave of compaction (i. e., the shock-wave transition of pores into the collapse state) are realized.

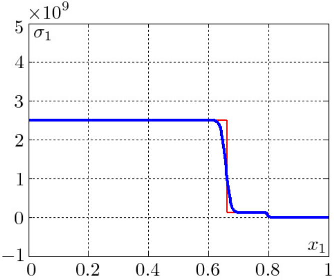

$\theta_0 = 5\,\%,\ \ p_0 = 75\,\tau_s$

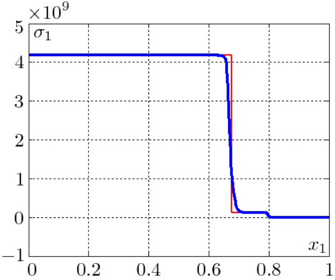

$\theta_0 = 5\,\%,\ \ p_0 = 125\,\tau_s$

Constant load at inner boundary of a rockhole

Distribution of computational load between nodes of a cluster

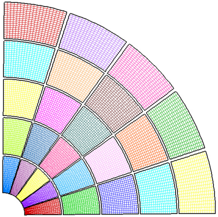

2D decomposition, 25 processors

Aluminum foam with a porosity of 1 %

Phenomenological parameters:
$\rho = 2673\,\mathrm{kg/m^3}$, $\tau_s = 0.0378\,\mathrm{MPa}$
$k_a = 71.58\,\mathrm{MPa}$, $\mu_a = 24.54\,\mathrm{MPa}$
$k_b = 4.256\,\mathrm{MPa}$, $\mu_b = 1.459\,\mathrm{MPa}$

The interior radius of pipe is 10 cm, its outer radius is 1 m

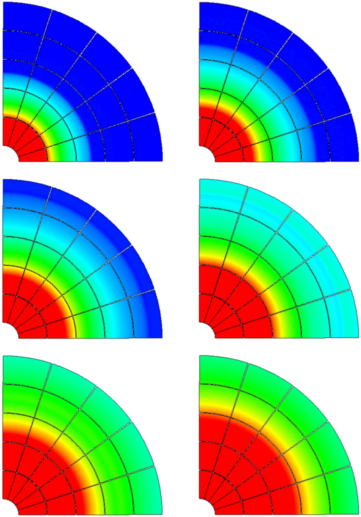

Level curves of plastic dissipation

Constant load at inner boundary of a rockhole

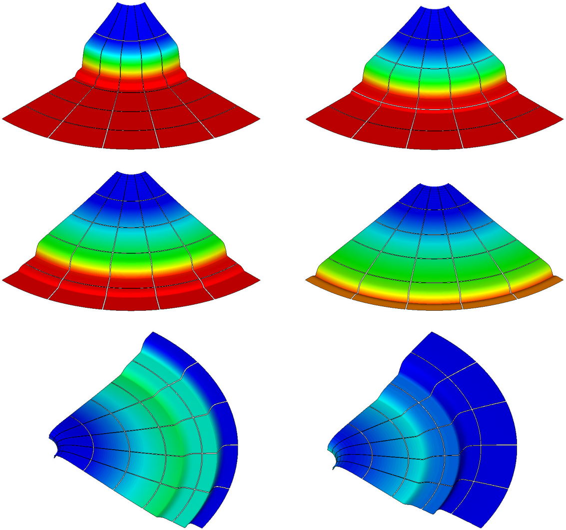

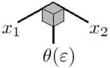

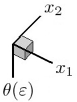

25 processors,
250 × 250 nodes

Fields of volumetric strain $\theta(\varepsilon)$

Concentrated impulsive load (Lamb problem)

Symmetric case

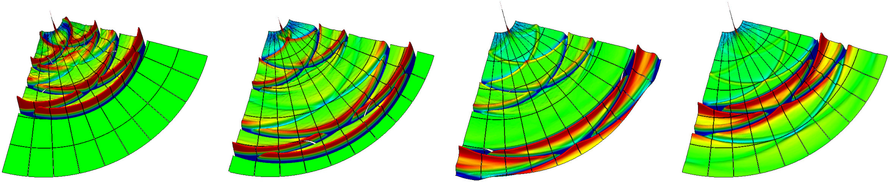

Fields of radial stress

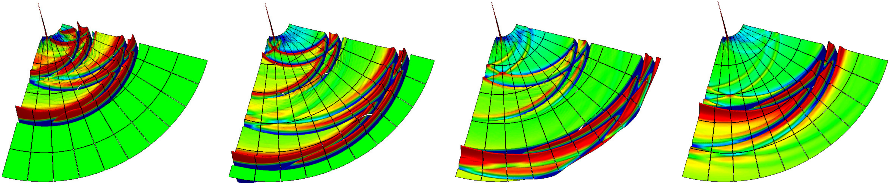

Nonsymmetric case

50 processors, 500×500 nodes

Periodic localized load

Waves, caused by periodic localized load at the inner boundary

Symmetric case

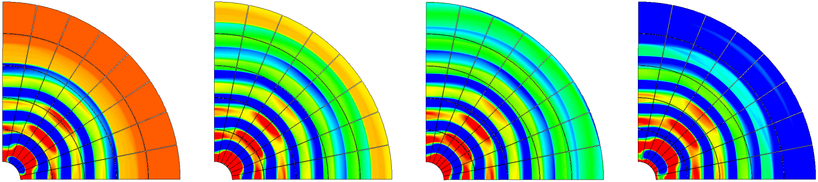

Level curves of volumetric strain $\theta(\varepsilon)$

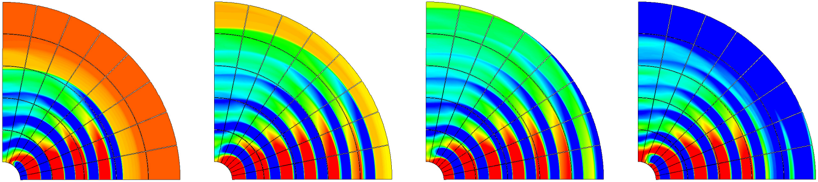

Nonsymmetric case

40 processors, 400×400 nodes

A blocky model of geological media

The faults and/or filed fractures in the reservoir introduce a network, communicate hydraulically between each other locally and globally, and provide overall conductivity (permeability) of the reservoir, and the matrix provides overall storage capacity (porosity).

Dual-porosity reservoir model

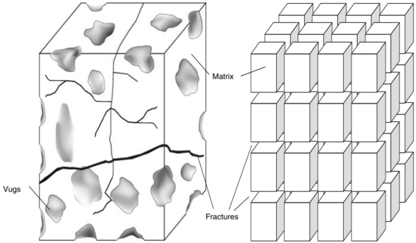

Fractured reservoir *Sugar cube representation*

Warren J.E., Root P.J. **The behavior of naturally fractured reservoirs. SPE J.** 1963. V. 3. P. 245–255.

Sadovskii M.A. **Natural lumpiness of a rock. Dokl. Akad. Nauk SSSR**. 1979. V. 247, No. 4. P. 829–831.

Equations of elastic blocks and elastic interlayers

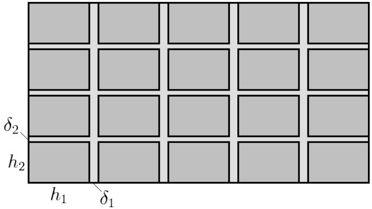

Scheme of a blocky medium

A motion of each block is defined by the system of equations of a homogeneous isotropic elastic medium:

$$\begin{aligned}
\rho\,\dot v_1 &= \sigma_{11,1} + \sigma_{12,2}\\
\rho\,\dot v_2 &= \sigma_{12,1} + \sigma_{22,2}\\
\dot\sigma_{11} &= \rho\,c_1^2\big(v_{1,1} + v_{2,2}\big) - 2\,\rho\,c_2^2\,v_{2,2}\\
\dot\sigma_{22} &= \rho\,c_1^2\big(v_{1,1} + v_{2,2}\big) - 2\,\rho\,c_2^2\,v_{1,1}\\
\dot\sigma_{12} &= \rho\,c_2^2\big(v_{2,1} + v_{1,2}\big)
\end{aligned}$$

Elastic interlayer between the horizontally located nearby blocks is described by the system of equations:

$$\rho'\,\frac{\dot v_1^+ + \dot v_1^-}{2} = \frac{\sigma_{11}^+ - \sigma_{11}^-}{\delta_1}, \qquad \frac{\dot\sigma_{11}^+ + \dot\sigma_{11}^-}{2} = \rho'\,{c_1'}^2\,\frac{v_1^+ - v_1^-}{\delta_1}$$

$$\rho'\,\frac{\dot v_2^+ + \dot v_2^-}{2} = \frac{\sigma_{12}^+ - \sigma_{12}^-}{\delta_1}, \qquad \frac{\dot\sigma_{12}^+ + \dot\sigma_{12}^-}{2} = \rho'\,{c_2'}^2\,\frac{v_2^+ - v_2^-}{\delta_1}$$

Elastic interlayer between the vertically located nearby blocks is modeled using similar system:

$$\rho'\,\frac{\dot v_2^+ + \dot v_2^-}{2} = \frac{\sigma_{22}^+ - \sigma_{22}^-}{\delta_2}, \qquad \frac{\dot\sigma_{22}^+ + \dot\sigma_{22}^-}{2} = \rho'\,{c_1'}^2\,\frac{v_2^+ - v_2^-}{\delta_2}$$

$$\rho'\,\frac{\dot v_1^+ + \dot v_1^-}{2} = \frac{\sigma_{12}^+ - \sigma_{12}^-}{\delta_2}, \qquad \frac{\dot\sigma_{12}^+ + \dot\sigma_{12}^-}{2} = \rho'\,{c_2'}^2\,\frac{v_1^+ - v_1^-}{\delta_2}$$

Elastic-plastic interlayers

To take into account the plasticity, constitutive equations of the vertical elastic interlayer are replaced by the variational inequality:

$$(\delta\sigma_{11}^{+} + \delta\sigma_{11}^{-})\,\dot\varepsilon_{11}^{p} + (\delta\sigma_{12}^{+} + \delta\sigma_{12}^{-})\,\dot\varepsilon_{12}^{p} \leqslant 0$$

$\delta\sigma_{jk}^{\pm} = \tilde\sigma_{jk}^{\pm} - \sigma_{jk}^{\pm}$ – variations of stresses

$\dot\varepsilon_{11}^{p} = \dfrac{v_1^{+} - v_1^{-}}{\delta_1} - \dfrac{\dot\sigma_{11}^{+} + \dot\sigma_{11}^{-}}{2\,\rho'\,{c'_1}^2}, \quad \dot\varepsilon_{12}^{p} = \dfrac{v_2^{+} - v_2^{-}}{\delta_1} - \dfrac{\dot\sigma_{12}^{+} + \dot\sigma_{12}^{-}}{2\,\rho'\,{c'_2}^2}$ – plastic strain rates

The actual stresses $\sigma_{jk}^{\pm}$ and variable stresses $\tilde\sigma_{jk}^{\pm}$ are subjected to the constraint in the form:

$$f\left(\frac{\tilde\sigma_{11}^{+} + \tilde\sigma_{11}^{-}}{2}, \frac{\tilde\sigma_{12}^{+} + \tilde\sigma_{12}^{-}}{2}\right) \leqslant \tau(\chi)$$

τ – material yield point of interlayers, χ – material parameter (or set of parameters) of hardening
$f(\sigma_n, \sigma_\tau)$ – equivalent stress function, in which arguments are normal and tangential stresses

The simplest form of the constraint for a microfractured medium is as follows:

$|\sigma_\tau| \leqslant \tau_s - k_s\,\sigma_n \qquad$ (τ_s and k_s – material parameters)

Constitutive equations of the horizontal elastic-plastic interlayer are formulated in a similar way

Poynting–Thomson's viscoelastic model

To describe the viscous dissipative effects in the interlayers under shear stresses, the Poynting–Thomson model of a viscoelastic medium is used.

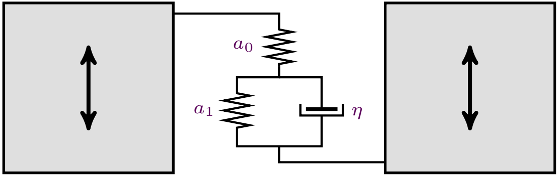

Poynting–Thomson's rheological scheme

Hooke's law for elastic element: $\varepsilon'_{12} = a_0\,(\sigma^+_{12} + \sigma^-_{12})/2, \quad \varepsilon''_{12} = a_1 s_{12}$

Newton's law for viscous element: $\eta\,\dot\varepsilon''_{12} = (\sigma^+_{12} + \sigma^-_{12})/2 - s_{12}$ Total strain: $\varepsilon_{12} = \varepsilon'_{12} + \varepsilon''_{12}$

Constitutive equations of the interlayer:

$$a_0\,\frac{\dot\sigma^+_{12} + \dot\sigma^-_{12}}{2} + a_1\,\dot s_{12} = \frac{v^+_2 - v^-_2}{\delta_1}, \qquad \frac{\sigma^+_{12} + \sigma^-_{12}}{2} = s_{12} + \eta\,a_1\,\dot s_{12}$$

Energy balance equation:

$$\frac{\sigma^+_{12} + \sigma^-_{12}}{2}\,\frac{v^+_2 - v^-_2}{\delta_1} = \dot W + \eta\,a_1^2\,\dot s_{12}^2, \quad 2\,W = a_0\,\frac{(\sigma^+_{12} + \sigma^-_{12})^2}{4} + a_1\,s_{12}^2$$

according to which the power of internal stresses in the interlayer is the sum of the reversible elastic strain power and the power of the viscous energy dissipation

Model of porous interlayers

The longitudinal deformation of the interlayers is described on the basis of a complicated version of the porous elastic model, which takes into account the strength increasing during the collapse of pores.

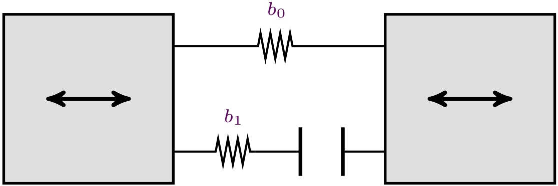

Rheological scheme of a porous interlayer

Total strain: $\varepsilon_{11} = \sigma'_{11}/b_1 + \theta_1 - \theta_0$

$\sigma'_{11} \leqslant 0$ – stress in a rigid contact, $\theta_0 > 0$ and $\theta_1 \geqslant 0$ – initial and current porosity values

Governing relations of a rigid contact: $(\tilde{\sigma}_{11} - \sigma'_{11})\,\theta_1 \leqslant 0, \quad \tilde{\sigma}_{11},\, \sigma'_{11} \leqslant 0$

$\sigma'_{11} = b_1\,\pi(\theta_0 + \varepsilon_{11}),\ \ \pi(\theta) = \min(\theta, 0)$ – projection onto the non-positive semi-axis

Constitutive equations of the interlayer including the equation for porosity:

$$\dot{\varepsilon}_{11} = \frac{v_1^+ - v_1^-}{\delta_1}, \quad \frac{\sigma_{11}^+ + \sigma_{11}^-}{2} = b_0\,\varepsilon_{11} + b_1\,\pi(\theta_0 + \varepsilon_{11}), \quad \theta_1 = \theta_0 + \varepsilon_{11} - \pi(\theta_0 + \varepsilon_{11})$$

The energy balance equation: $\dfrac{\sigma_{11}^+ + \sigma_{11}^-}{2}\,\dot{\varepsilon}_{11} = \dot{W}, \quad 2\,W = b_0\,\varepsilon_{11}^2 + b_1\,\pi^2(\theta_0 + \varepsilon_{11})$

Modified Biot's model

Under numerical modeling of the wave motion in a blocky medium containing fluid-saturated porous interlayers, a version of the model is applied based on Biot's approach.

Kinetic energy related to the initial unit of a volume of the horizontal interlayers:

$$2\,T = \rho_s\,\frac{(v_1^+ + v_1^-)^2}{4} + \rho_a\Big(\frac{v_1^+ + v_1^-}{2} - w_1\Big)^2 + (\rho_s + \rho_f)\,\frac{(v_2^+ + v_2^-)^2}{4} + \rho_f\,w_1^2$$

ρ_s, ρ_f – partial densities of a solid skeleton and a liquid phase in interlayers at the initial moment of time
ρ_a – density of additional mass used to take into account the mutual influence of fluid and skeleton in the case of relative motion, w_1 – absolute velocity of the fluid motion

Equations describing skeleton motion in the direction of longitudinal axis x_1:

$$(\rho_s + \rho_a)\,\frac{\dot v_1^+ + \dot v_1^-}{2} - \rho_a\,\dot w_1 = \frac{\sigma_{12}^+ - \sigma_{12}^-}{\delta_2}$$

$$a_0\,\frac{\dot\sigma_{12}^+ + \dot\sigma_{12}^-}{2} + a_1\,\dot s_{12} = \frac{v_1^+ - v_1^-}{\delta_2}, \qquad \frac{\sigma_{12}^+ + \sigma_{12}^-}{2} = s_{12} + \eta\,a_1\,\dot s_{12}$$

Equations describing joint motion of the solid and liquid phase in the direction of transverse axis x_2:

$$(\rho_s + \rho_f)\,\frac{\dot v_2^+ + \dot v_2^-}{2} = \frac{\sigma_{22}^+ - \sigma_{22}^-}{\delta_2}, \quad \dot\varepsilon_{22} = \frac{v_2^+ - v_2^-}{\delta_2}, \quad \frac{\dot\sigma_{22}^+ + \dot\sigma_{22}^-}{2} = b_0\,\dot\varepsilon_{22} + b_1\,\dot\pi(\theta_0 + \varepsilon_{22}) + b_s\,w_{1,1}$$

Equations describing the fluid motion along the interlayer:

$$(\rho_f + \rho_a)\,\dot w_1 - \rho_a\,\frac{\dot v_1^+ + \dot v_1^-}{2} = s_{11,1}, \quad \dot s_{11} = b_f\,w_{1,1} + b_s\,\dot\varepsilon_{22}$$

$s_{11} = -p\,\theta$ – normal stress in the liquid phase, p – value of the pore pressure
θ – momentary porosity value, b_s and b_f – elastic moduli characterizing the interaction in the system "solid skeleton–fluid"

Kirchhoff's law for nodes

To solve the systems numerically, the computational algorithm is developed. The Godunov gap decay scheme is applied at the stage of approximation of the equations for velocity w_1 and stress s_{11} in a fluid.

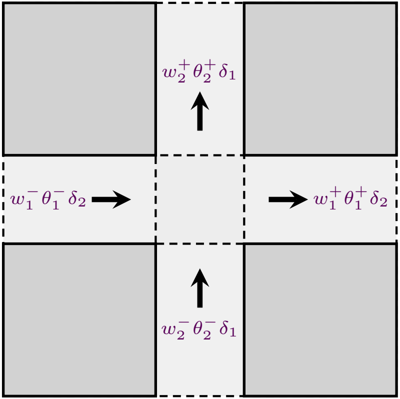

Scheme of flows interaction

At junction zones of the horizontal and vertical interlayers, the internal boundary conditions are set.

They result from Kirchhoff's law for the fluid flow:

$$w_1^+\,\theta_1^+\,\delta_2 + w_2^+\,\theta_2^+\,\delta_1 = w_1^-\,\theta_1^-\,\delta_2 + w_2^-\,\theta_2^-\,\delta_1$$

and the dynamic equations:

$$s_{11}^{\pm} = -p\,\theta_1^{\pm}, \quad s_{22}^{\pm} = -p\,\theta_2^{\pm}$$

considering the pressure equality at a junction.

$\theta_1^{\pm}$ and $\theta_2^{\pm}$ – porosities in the horizontal and vertical interlayers

In this formulation of the boundary conditions at the junctions, the power balance equation is fulfilled:

$$s_{11}^+\,w_1^+\,\delta_2 + s_{22}^+\,w_2^+\,\delta_1 - s_{11}^-\,w_1^-\,\delta_2 - s_{22}^-\,w_2^-\,\delta_1 = 0$$

which guaranteed the thermodynamic consistency of equations in the inner layers and blocks.

Model of separation cracks

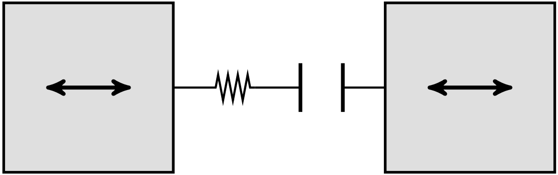

Rheological scheme of contact interaction of crack edges

Conditions of contact interaction of the crack edges are formulated as a variational inequality

$$\delta\sigma_{11}\left(\frac{1}{\rho' c_1'^2}\,\sigma_{11}-\varepsilon_{11}\right)\geqslant 0,\qquad \dot{\varepsilon}_{11}=\frac{v_1^+-v_1^-}{\delta_1}$$

The algorithm of numerical implementation in a mesh of a grid is based on the equations

$$\hat{\varepsilon}_{11}=\varepsilon_{11}+\frac{v_1^+-v_1^-}{\delta_1}\,\tau,\qquad z_1 v_1^+ +\sigma_{11}^+=R_1^+,\qquad z_1 v_1^- -\sigma_{11}^-=R_1^-$$

and the closing equation $\hat{\sigma}_{11}+\sigma_{11}=\sigma_{11}^+ +\sigma_{11}^-$, guaranteeing the absence of artificial dissipation of energy, which gives the procedure of stress correction

$$\hat{\sigma}_{11}=\frac{1}{\kappa}\,\pi_-\left(\varepsilon_{11}+\frac{R_1^+-R_1^- -\sigma_{11}}{z_1\delta_1}\,\tau\right),\qquad \kappa=\frac{1}{\rho' c_1'^2}+\frac{\tau}{\rho\, c_1\delta_1}$$

Two-cyclic splitting

We developed parallel computational algorithm for supercomputers of the cluster architecture based on a two-cyclic method of splitting, which has high accuracy and permits the efficient parallelization of computations.

Governing equations in blocks and interlayers are represented in the form of symbolic evolution equation:

$$\dot{U} = A_1(U) + A_2(U)$$

A_1 and A_2 – nonlinear differential-difference operators, simulating 1D motion of a blocky medium in the direction of the coordinate axes x_1 and x_2, U – vector–function of unknown quantities which includes the projection of the velocity vector and the stress tensor in blocks and interlayers

The method of splitting on the time interval $(t_0, t_0 + \Delta t)$ includes four steps: the step of solving 1D equation in the x_1 direction on the interval $(t_0, t_0 + \Delta t/2)$, a similar step of solving the equation in the x_2 direction, the step of recomputation in the x_2 direction on the interval $(t_0 + \Delta t/2, t_0 + \Delta t)$ and the step of recomputation in the x_1 direction on the same interval:

$$\begin{aligned}
\dot{U}^{(1)} &= A_1(U^{(1)}), \quad U^{(1)}(t_0) = U(t_0)\\
\dot{U}^{(2)} &= A_2(U^{(2)}), \quad U^{(2)}(t_0) = U^{(1)}(t_0 + \Delta t/2)\\
\dot{U}^{(3)} &= A_2(U^{(3)}), \quad U^{(3)}(t_0 + \Delta t/2) = U^{(2)}(t_0 + \Delta t/2)\\
\dot{U}^{(4)} &= A_1(U^{(4)}), \quad U^{(4)}(t_0 + \Delta t/2) = U^{(3)}(t_0 + \Delta t)
\end{aligned}$$

The solution at the time instant $t_0 + \Delta t$ equals to $U(t_0 + \Delta t) = U^{(4)}(t_0 + \Delta t)$

Efficiency of parallelization

Computational algorithm is implemented as the parallel program for analysis of the waves propagation processes in blocky media under external dynamic loads. The parallelization is performed on the basis of domain decomposition – each processor of a cluster expects a separate chain of blocks including the boundary interlayers in the horizontal direction. The programming language is Fortran, and the message passing interface (MPI) library is used.

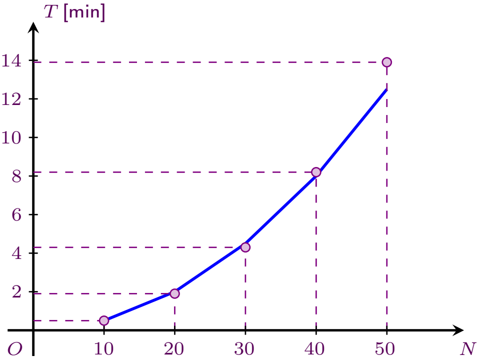

Dependence of the runtime T on the linear dimension N of a grid in blocks (circle points – actual computational time, solid line – semi-theoretical computational time)

Instant rotation of the central block in the rock mass

$\delta = 0.1$ mm $\qquad \delta = 1$ mm $\qquad \delta = 5$ mm

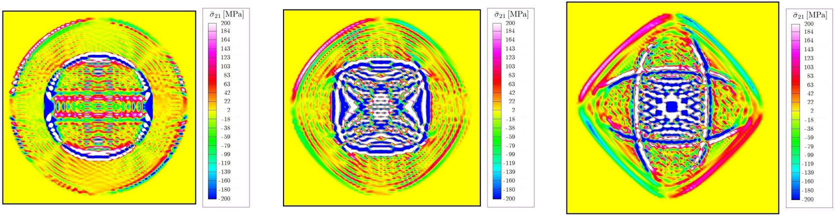

Level curves of the tangential stress depending on the thickness of interlayers

The case of porous interlayers

Rock massif consists of 100 x 100 blocks, size of each block is 50 mm x 50 mm

Sadovskii V.M., Sadovskaya O.V. **Modeling of elastic waves in a blocky medium based on equations of the Cosserat continuum.** **Wave Motion**. 2015. V. 52. P. 138–150.
DOI: 10.1016/j.wavemoti.2014.09.008
http://www.sciencedirect.com/science/article/pii/S0165212514001358

Sadovskii V.M., Sadovskaya O.V., Lukyanov A.A. **Modeling of wave processes in blocky media with porous and fluid-saturated interlayers.** **Journal of Computational Physics**. 2017. V. 345. P. 834–855. DOI: 10.1016/j.jcp.2017.06.001
http://www.sciencedirect.com/science/article/pii/S0021999117304461

Instant rotation of the central block in the rock mass

$\delta = 0.1$ mm $\delta = 1$ mm $\delta = 5$ mm

The case of elastic interlayers

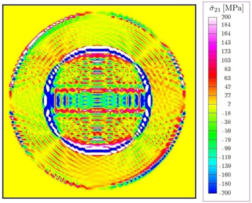

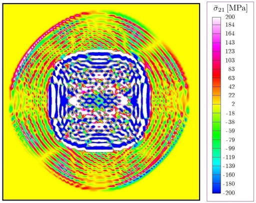

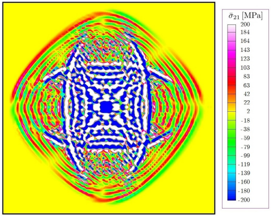

Level curves of the tangential stress depending on the thickness of interlayers

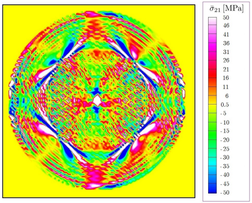

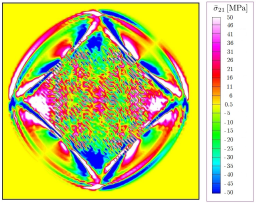

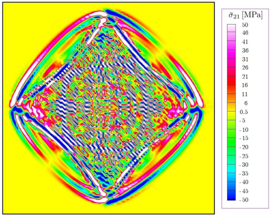

The case of elastic-plastic interlayers

Instant rotation of the central block in the rock mass

$\delta = 0.1\,\mathrm{mm}$ $\delta = 1\,\mathrm{mm}$ $\delta = 5\,\mathrm{mm}$

The case of porous interlayers: intensive load (with pore collapse)

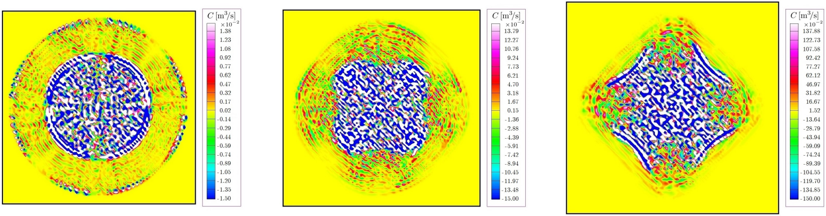

Level curves of the fluid circulation around blocks depending on the thickness of interlayers

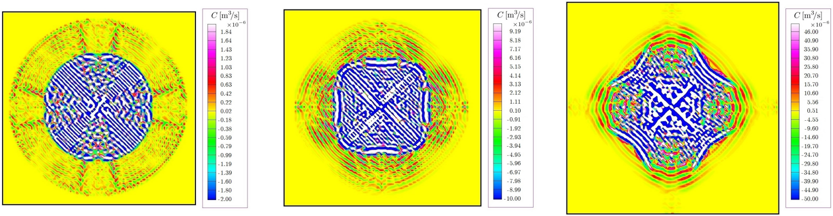

The case of porous interlayers: small load (without pore collapse)

Crack propagation in a blocky medium

The action of Π-shaped pulse load on a part of the upper boundary of a blocky massif

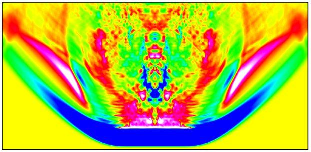

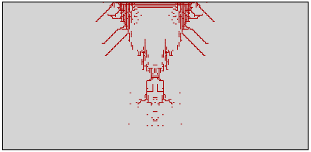

Level curves of the normal stress σ_{22}

Formation and propagation of the system of interblock cracks

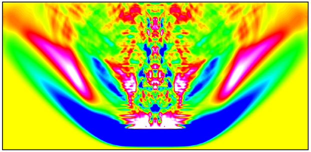

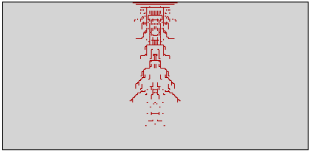

The action of Π-shaped smoothed pulse load on a part of the upper boundary of a blocky massif

100 layers, 200 blocks in each of them

100 nodes, 1D decomposition of computational domain

For plane strain, the equations of the Cosserat elastic continuum:

$$\rho_0\,\dot v_1 = \sigma_{11,1} + \sigma_{12,2}, \qquad \rho_0 \dot v_2 = \sigma_{21,1} + \sigma_{22,2}$$

$$J_0\,\dot\omega_3 = \mu_{31,1} + \mu_{32,2} + \sigma_{21} - \sigma_{12}$$

$$a_1\,\dot\sigma_{11} - b_1\,\dot\sigma_{22} = v_{1,1}, \qquad a_1\,\dot\sigma_{22} - b_1\,\dot\sigma_{11} = v_{2,2}$$

$$a_2\,\dot\sigma_{21} - b_2\,\dot\sigma_{12} = v_{2,1} - \omega_3$$

$$a_2\,\dot\sigma_{12} - b_2\,\dot\sigma_{21} = v_{1,2} + \omega_3$$

$$\dot\mu_{31} = \alpha_2\,\omega_{3,1}, \qquad \dot\mu_{32} = \alpha_2\,\omega_{3,2}$$

written in Cartesian coordinates relative to the linear velocities v_1, v_2, angular velocity ω_3, stresses σ_{jk} and couple stresses μ_{jk} can be represented in the matrix form:

$$A\,\frac{\partial U}{\partial t} = B^1\,\frac{\partial U}{\partial x_1} + B^2\,\frac{\partial U}{\partial x_2} + Q\,U$$

$$U = \Big(v_1,\, v_2,\, \omega_3,\, \sigma_{11},\, \sigma_{22},\, \sigma_{21},\, \sigma_{12},\, \mu_{31},\, \mu_{32}\Big)$$

with symmetric matrix–coefficients A, B^1, B^2 and antisymmetric matrix Q.

This system belongs to the class of symmetric t-hyperbolic systems by Friedrichs and systems of thermodynamically consistent conservation laws by Godunov.

Elastic-plastic Cosserat continuum

It is possible to construct a model of Cosserat elastoplastic continuum on the basis of the system of equations of the theory of elasticity. Such a model is formulated as a variation inequality

$$(\tilde{U} - U) \cdot \left(A \frac{\partial U}{\partial t} - B^1 \frac{\partial U}{\partial x_1} - B^2 \frac{\partial U}{\partial x_2} - Q\,U \right) \geqslant 0, \qquad \tilde{U},\, U \in F$$

Here F is the set of admissible variations of the vector U, $\tilde{U}$ is an arbitrary element of F.

This variational inequality is a formulation of the Mises principle of maximum power of plastic dissipation. The boundary of F in the space of stress and couple stress tensors is the yield surface of material, which is equivalent to the system of constitutive equations of plasticity in the form of associative flow role.

Sadovskii V.M. **Discontinuous Solutions in Dynamic Elastic–Plastic Problems.** Physics and Mathematics Literature Publishing Company, Moscow, 1997. 208 p. (in Russian)

Sadovskaya O., Sadovskii V. **Mathematical Modeling in Mechanics of Granular Materials.** Ser.: **Advanced Structured Materials**, Vol. 21. Springer, Heidelberg – New York – Dordrecht – London, 2012. 390 p. DOI: 10.1007/978-3-642-29053-4

http://link.springer.com/book/10.1007/978-3-642-29053-4

Plasticity in interlayers

Since the behavior of continuum is completely determined by the deformation properties of the weakened interlayers of blocky structure, the yield criterion is used in the form

$$|\sigma_{21}| \leqslant \tau_0 - \kappa_\tau\, \sigma_{11}, \qquad |\sigma_{12}| \leqslant \tau_0 - \kappa_\tau\, \sigma_{22}$$

$$|\mu_{31}| \leqslant \mu_0 - \kappa_\mu\, \sigma_{11}, \qquad |\mu_{32}| \leqslant \mu_0 - \kappa_\mu\, \sigma_{22}$$

It limits the tangential stresses, which characterize shifts along the interlayers, and couple stresses, the attainment of which limit values lead to an irreversible change in the curvature.

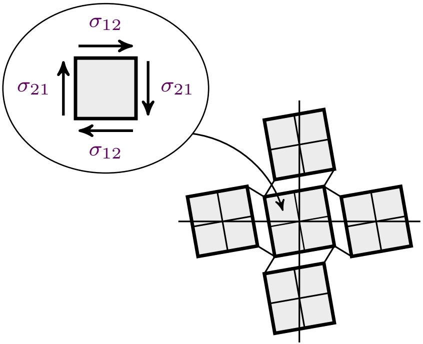

Tangential stresses caused by rotations of the blocks

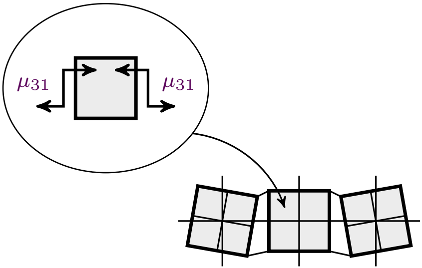

Scheme of couple-stressed interactions

U-shaped pulse loading

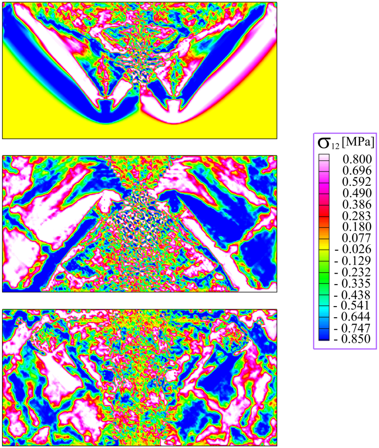

Level curves of tangential stress σ_{12}

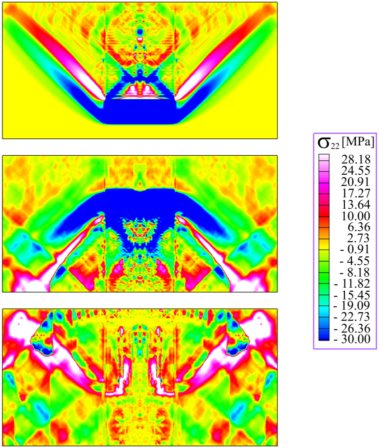

Level curves of normal stress σ_{22}

U-shaped pulse loading

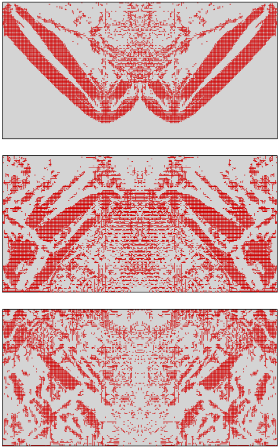

Configuration of plastic zones

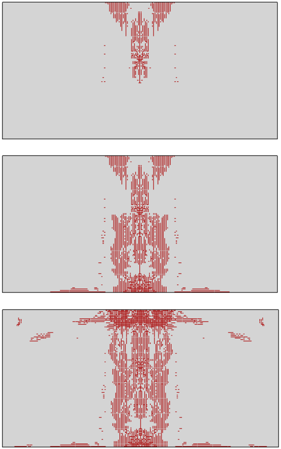

Configuration of fracture zones

Λ-shaped pulse loading

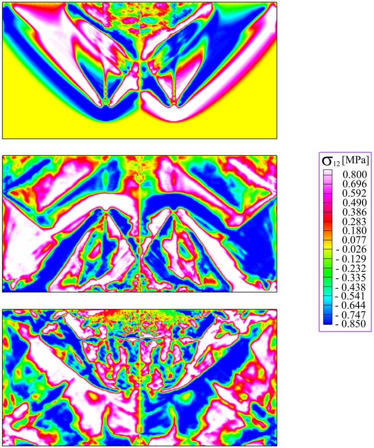

Level curves of tangential stress σ_{12}

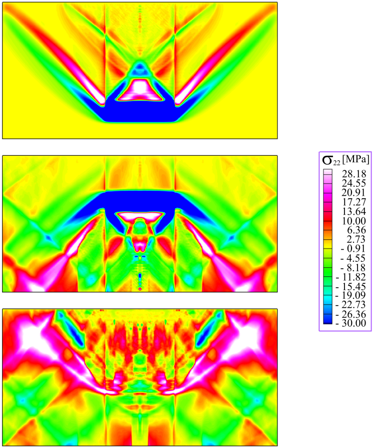

Level curves of normal stress σ_{22}

Λ-shaped pulse loading

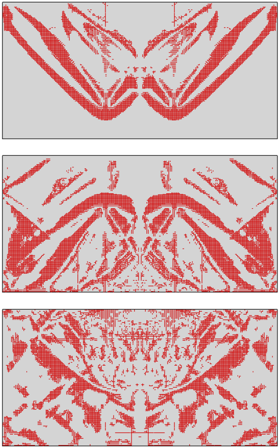

Configuration of plastic zones

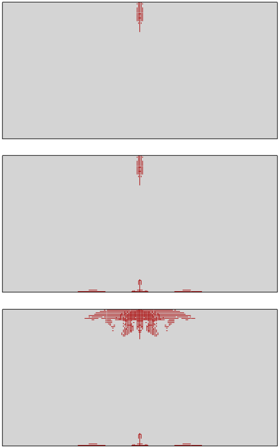

Configuration of fracture zones

U-shaped pulse without fracture

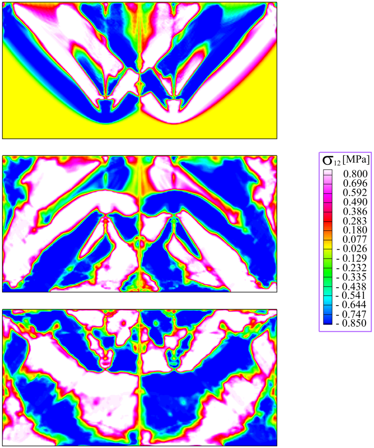

Level curves of tangential stress σ_{12}

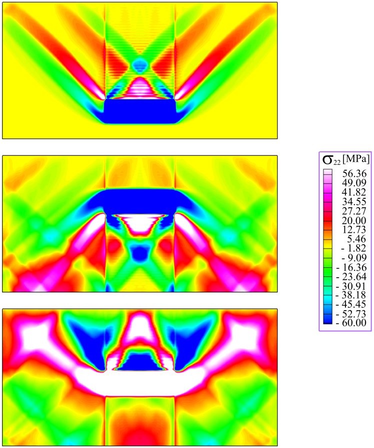

Level curves of normal stress σ_{22}

U-shaped pulse without fracture

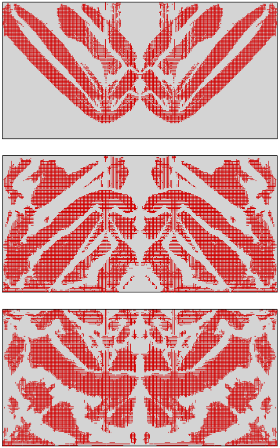

Configuration of plastic zones

U-shaped pulse loading: Cosserat model

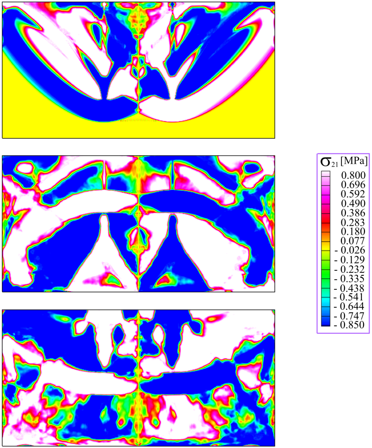

Level curves of tangential stress σ_{12}

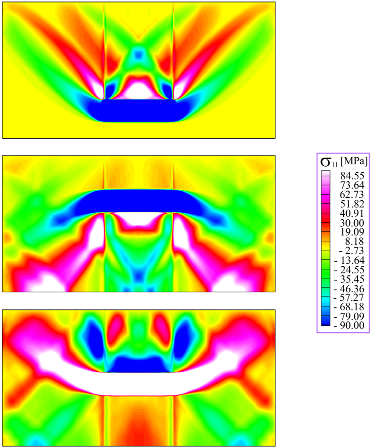

Level curves of normal stress σ_{22}

U-shaped pulse loading: Cosserat model

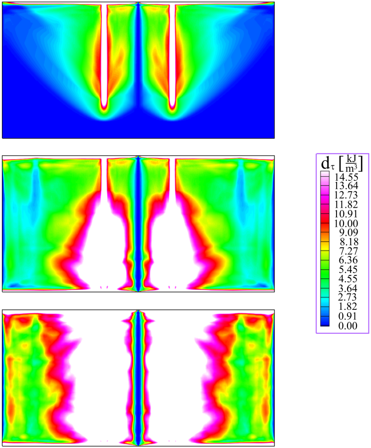

Level curves of plastic dissipative energy

U-shaped pulse loading: Cosserat model

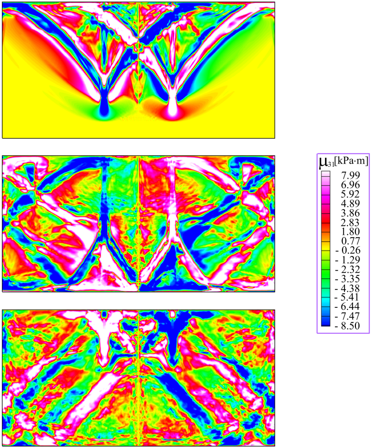

Level curves of couple stress μ_{31}

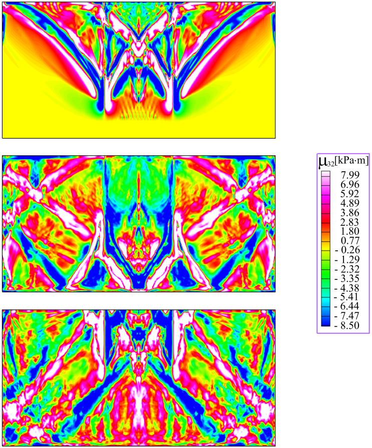

Level curves of couple stress μ_{32}

U-shaped pulse loading: Cosserat model

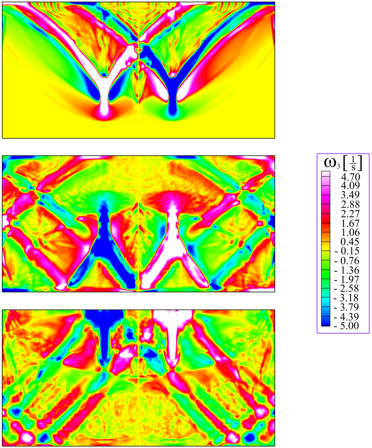

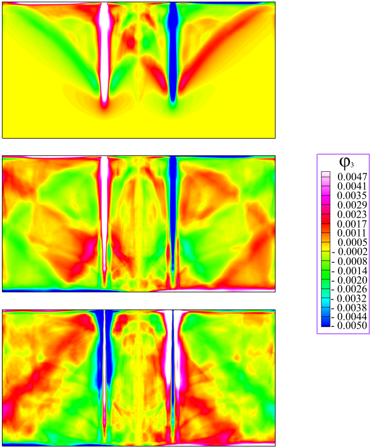

Level curves of angular velocity ω_3

Level curves of rotation angle φ_3 $(\dot{\varphi}_3 = \omega_3)$

Conclusions

- By means of a generalized rheological method we constructed the constitutive equations of granular and porous media, describing the nonlinear effect of strength increasing in a material after the collapse of pores.
- We worked out parallel computational algorithms and programs for numerical implementation of the dynamic models for structurally inhomogeneous media on supercomputers of cluster architecture.
- We carried out a series of numerical experiments on the elastic-plastic waves propagation in granular, blocky and porous geomaterials as well as on the resonance excitation in an elastic Cosserat medium at the natural frequency of the rotational motion of particles.

The reported study was funded by the Russian Foundation for Basic Research, Government of Krasnoyarsk Territory, Krasnoyarsk Regional Fund of Science to the research project No. 18-41-242001

Many thanks for your attention and for your interest !!!